

Mechanical and fracture behavior of cement-based materials characterized by combined elastic wave approaches



A.C. Mpalaskas^a, O.V. Thanasia^a, T.E. Matikas^a, D.G. Aggelis^{a,b,*}

^a Department of Materials Science and Engineering, University of Ioannina, 45110 Ioannina, Greece

^b Department of Mechanics of Materials and Constructions, Vrije Universiteit Brussel, Pleinlaan 2, 1050 Brussels, Belgium

HIGHLIGHTS

- Excellent agreement between experimental pulse velocity of concrete and theoretical results based on scattering models.
- Characterization of damage content based on wave propagation parameters.
- Correlation of acoustic emission parameters with strength.

ARTICLE INFO

Article history:

Received 2 April 2013

Received in revised form 2 September 2013

Accepted 14 October 2013

Keywords:

Acoustic emission

Damage

Mortar

Scattering

Ultrasound

ABSTRACT

In the present paper cementitious material with simulated damage is examined as to its mechanical and fracture properties. Nondestructive monitoring techniques are applied in an effort to establish or improve correlations with the simulated damage content and the failure load. Specifically, the specimens are ultrasonically interrogated before fracture, while during fracture their behavior is monitored by acoustic emission. Scattering theory seems adequate to explain the experimental ultrasonic behavior showing that modern approaches should incorporate the heterogeneity instead of considering the material macroscopically homogeneous. Apart from the strong correlations between wave velocity and damage content in the form of light inclusions, specific acoustic emission parameters show good correlation not only to simulated damage content but also to the ultimate bending load. Overall, the suitability of ultrasonic parameters to investigate damage and of acoustic emission parameters to correlate with failure load are discussed, while the influence of material's heterogeneity on the distortion of the signals is also discussed.

© 2013 Elsevier Ltd. All rights reserved.

1. Introduction

Reliable nondestructive evaluation (NDE) of material condition is a prerequisite for successful structural health monitoring (SHM). Wave propagation, commonly referred to as ultrasonic testing (UT) offers this nondestructive nature along with certain advantages. One of the strongest advantages is that wave velocity is directly connected to the elastic constants [1]. In most of the cases concrete can be considered macroscopically homogeneous and hence without large error, the elastic and shear moduli can be calculated. Additionally, numerous empirical correlations have already been proposed between elastic wave velocity (mainly longitudinal) and strength, being quite valuable for on-site evaluations [2]. Quite recently the heterogeneity of concrete and other materials have

started to be considered in order to explain more accurately phenomena like dispersion and attenuation [3–7]. Aggregates, porosity and especially air bubbles or damage in the form of cracking or light inclusions act as scatterers deflecting the wave beam. This introduces excessive scattering attenuation, and imposes a frequency dependent velocity behavior, as will be discussed.

Another utilization of elastic waves is in the framework of acoustic emission (AE) studies. In this case, no external wave excitation is applied but the elastic waves are emitted by fracture incidents inside the material under loading [8]. These waves carry information on the source of the fracture events and after recording and suitable study, characterization of the damage stage and mode is possible, especially in laboratory conditions [9–12]. However, due to their elastic nature, acoustic emission waves are similarly influenced by the heterogeneity of the medium, as any ultrasonic wave. Therefore, their energy, frequency content and general waveform shape changes as they propagate from the source to the receiver which is usually placed on the material's surface. Analysis of the AE parameters can well be used to characterize

* Corresponding author at: Department of Mechanics of Materials and Constructions, Vrije Universiteit Brussel, Pleinlaan 2, 1050 Brussels, Belgium. Tel.: +32 (0)2 6293541.

E-mail address: daggelis@vub.ac.be (D.G. Aggelis).

the damage process of brittle materials but simultaneously, care should be taken for the scattering influence on the signals [13,14].

In the present study both elastic wave techniques are applied in the characterization of cementitious mortar. Different volume contents of light nearly-spherical grains are included to simulate micro-cracking that could be the result of thermal damage. The spherical size of the inclusions make them suitable to simulate the randomly oriented micro-cracks as has been shown in cementitious and other material [15–18]. The material is ultrasonically interrogated in order to check the effect of inclusion content on the measured velocity of both longitudinal and surface wave modes. The density of the expanded polystyrene grains used as simulated damage, is an order of magnitude lower than the density of mortar, resulting in a strong acoustic impedance mismatch with the matrix, while the scattering contribution of sand grains is considered weak due to similar stiffness and density to the cement matrix. The results are compared with the prediction of scattering formulation of the problem of cavities inside an elastic matrix showing that the existence of damage is responsible for the observed behavior. Furthermore, and since strength is the most important property of a material from the engineering point of view, the specimens are fractured and their AE behavior is monitored. The effect of simulated damage is very strong on the AE signals as well, since several monotonic and innovative correlations are observed between AE parameters and damage content. Additionally, specific AE parameters exhibit strong correlations to the bending tensile strength since the latter is firmly connected to the fracture events occurring inside the material which give rise to the recorded emissions. Although the empirical relation between ultrasound and (mainly compressive) strength is well known, there is no theoretically justified relation between the elastic constants and strength. Strength depends on fracture mechanisms acting at the tip of cracks even in the micro-level which are not possible to critically affect wave propagation of elastic wave lengths several orders of magnitude longer. On the other hand even the smallest fracturing event emits an amount of energy that can trigger its acquisition by the AE transducers. Therefore, parameters evolving from UT and AE testing are related to both mechanical and fracture properties. After proper combined study, the different techniques may act complementarily in evaluation of different parameters related to the material's performance, like heterogeneity content and failure load.

2. Experimental

2.1. Materials and testing

Seven different mortar mixtures were produced consisting of three specimens each. One was plain mortar (PM, including cement sand and water) and the others additionally included 1.5%, 2.5%, 5.0%, 7.5%, 10.0% and 12.5% (vol.) of light nearly-spherical expanded polystyrene inclusions (see Fig. 1) acting as voids. The average inclusions size was 3.9 mm as measured from a population of 20 particles. Sand grains were of 4.75 mm maximum size, while the water to cement ratio was 0.70 by mass. The density and the water absorption of the sand were 2500 kg/m^3 and 2.44% respectively. The exact mix proportions of PM were as follows: cement type (II 42.5 N) 440 kg/m^3 , water 308 kg/m^3 , sand $1,364 \text{ kg/m}^3$, super-plasticizer 4.5 kg/m^3 . For mortar with simulated damage the corresponding amount of inclusions was added in the mixer to account for the prescribed volume content, while the other parameters were modified accordingly so that to keep water to cement and sand to cement ratios constant. An idea of the microstructure at the scale of the inclusions, air bubbles and grains is shown in the photograph of Fig. 2 where the cross section of a specimen with 12.5% inclusions is included. No conglomeration of inclusions was noticed in any of the specimens after saw cutting at the end of the experiments.

The specimens were cured in water for 28 days prior to nondestructive and destructive testing. Their size was $40 \times 40 \times 160 \text{ mm}$ and they were eventually subjected to three-point bending according to EN 13892-2:2002 (Fig. 3a). The load was applied at a constant rate of 50 N/s until fracture and the loading was automatically terminated at the moment of load drop. Table 1 includes main physical and mechanical properties of the different materials.



Fig. 1. Particles used as simulated damage.

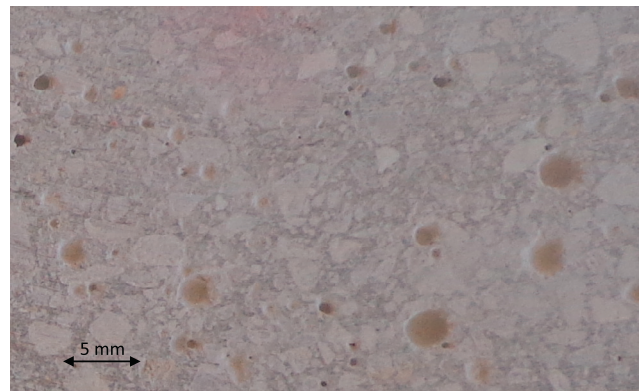


Fig. 2. Photograph of cross section for a mortar specimen with 12.5% of inclusions.

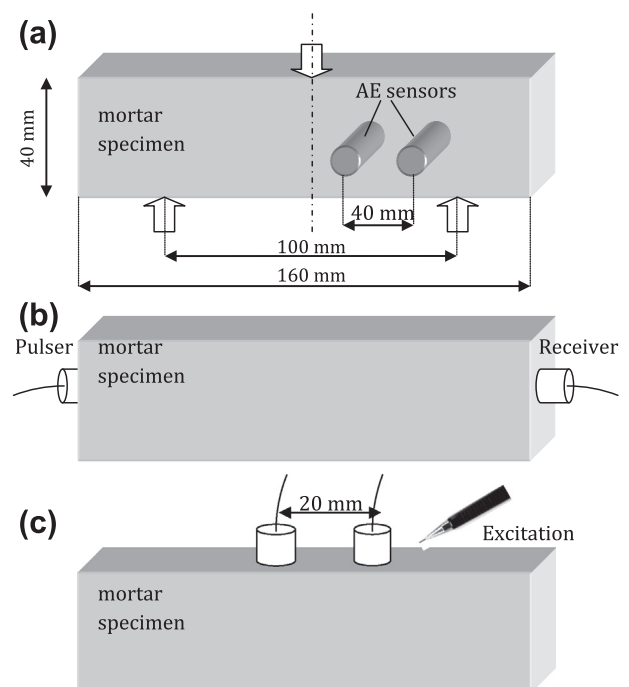


Fig. 3. Schematic representation of (a) three point bending test with AE monitoring, (b) ultrasonic test with longitudinal waves, and (c) ultrasonic test for surface waves.

Table 1
Basic physical and mechanical properties of the mixes (average of three specimens).

Mix name	Inclusions content (vol.%)	Density (kg/m ³)	Max. bending load (kN)	Longitudinal velocity (m/s)	Rayleigh velocity (m/s)	Elastic ^a modulus (GPa)
A	0	1969	2.92	3693	1960	24.4
B	1.5	1941	2.67	3684	1966	24.7
C	2.5	1821	2.55	3684	1891	22.6
D	5	1959	2.75	3582	1854	22.5
E	7.5	1914	2.36	3569	1893	22.6
F	10	1921	3.01	3545	1848	22.4
G	12.5	1880	2.22	3390	1729	18.9

^a Calculated from the longitudinal wave velocity and density.

2.2. Nondestructive monitoring

As to AE monitoring, which was conducted during the bending test, two AE sensors (Pico, PAC) were attached to the front side of the specimen as seen in Fig. 3a. They are considered quite broadband with central frequency of 500 kHz. Roller bearing grease was used for acoustic coupling, while the sensors were secured by the use of tape during the experiment. The horizontal distance between the sensors was 40 mm and the first was placed at the horizontal distance of 15 mm from the center where the crack was expected, as seen in Fig. 3a. The sensors were placed from the same side of the specimen, in order to be able in future to correlate the AE values with the traveled distance between the source crack (mid span) and the sensor. The signals were recorded in a two-channel monitoring board PCI-2, PAC with a sampling rate of 5 MHz. The threshold was set to 40 dB in order to avoid ambient noise and the acquired signals were pre-amplified by 40 dB.

Before the fracture test, the specimens were also ultrasonically examined both through the thickness (longitudinal mode) and on the surface (Rayleigh mode). The measurements were conducted by acoustic emission transducers (R15, PAC) which exhibit maximum sensitivity around 150 kHz and have a diameter of 15 mm. For the longitudinal wave examination (see Fig. 3b), the electric pulse fed to the transducer acting as pulser was one cycle of 150 kHz. The received signal was pre-amplified by 40 dB and digitized with a sampling rate of 10 MHz. Noise level was low and therefore, pulse velocity was measured by the first detectable disturbance of the waveform (onset). Due to the finite number of specimens (seven mixes of three specimens each) the onset was manually picked. The first disturbance corresponds to the longitudinal waves which are the fastest type. The length of the specimens (160 mm) over the pure wave transit time (after sensor delay effects are excluded) resulted in the pulse velocity for each measurement.

Concerning the Rayleigh mode, the excitation was introduced by a pencil lead break and the response at two positions on the surface was recorded again by R15 sensors (see Fig. 3c). Although the onset of the Rayleigh wave cannot be determined as it is masked by the faster longitudinal wave, the velocity is measured by a reference peak of Rayleigh in both waveforms which is much stronger than longitudinal [19–21].

3. Theoretical prediction

Due to the strong acoustic impedance mismatch between the stiff cementitious matrix and the light inclusions, and the relation between the applied wave length and inclusion size as will be discussed later, scattering is the first reasonable approach to explain the wave behavior of this material. Specifically the impedance of the mortar matrix is approximately 8 MRayl (with pulse velocity 4000 m/s and density of 2000 kg/m³). For the inclusions, pulse velocity values were not found in literature while their density is less than 100 kg/m³). In order to investigate the influence of the light inclusions on ultrasonic parameters, the simple multiple scattering theory of Waterman and Truell [22] is employed, which is an advancement of the model proposed by Foldy [23]. Application of this theory to concrete is well documented in the literature [3,4,24,25] so only a short introduction will take place herein.

A pulse propagating in a particulate composite or material with cavities undergoes both dispersion and attenuation due to its interaction with the embedded particles. According to the above mentioned model, this wave dispersion and attenuation is represented by a frequency-dependent complex wavenumber, k , which is expressed in terms of the particle concentration, ϕ , and the forward, $f(0)$, and the backward far-field, $f(\pi)$ scattering amplitudes:

$$\left(\frac{k}{k_c}\right)^2 = 1 + \frac{3\phi}{k_c^2 R^3} f(0) + \frac{9\phi^2}{4k_c^4 R^6} [f^2(0) - f^2(\pi)] \quad (1)$$

where in the above equation, R is the size of the scatterer and k_c is the wave number of the matrix.

The scattering amplitudes $f(0)$ and $f(\pi)$ are taken from the solution of the single particle wave scattering problem where a plane wave of given frequency impinges upon a particle/cavity suspended in the matrix. The single scattering parameters required are evaluated by means of the corresponding analytical expressions provided by Ying and Truell [26]. Using this formulation, the problem of a longitudinal plane wave impinging on a spherical obstacle is dealt with, taking into account the continuity of displacements and stresses on the scatterer–matrix interface. A schematic representation of the two addressed problems is depicted in Fig. 4a for single and Fig. 4b for multiple scattering. The velocity of the scattered wave is of interest, while the incident wave is a monochromatic wave with user-selected frequency. Practically the procedure is repeated for as many frequencies the user selects. In this case results up to 400 kHz were obtained. For each different radial frequency ω , the complex wave number, k , is calculated through (1) and the phase velocity is derived from the real part of the wave number, k :

$$K = \frac{\omega}{c} + i\alpha \quad (2)$$

while the attenuation coefficient α is the imaginary part.

For the specific calculations the elastic modulus used for the cement matrix is 24.4 GPa as measured by ultrasonic test in plain

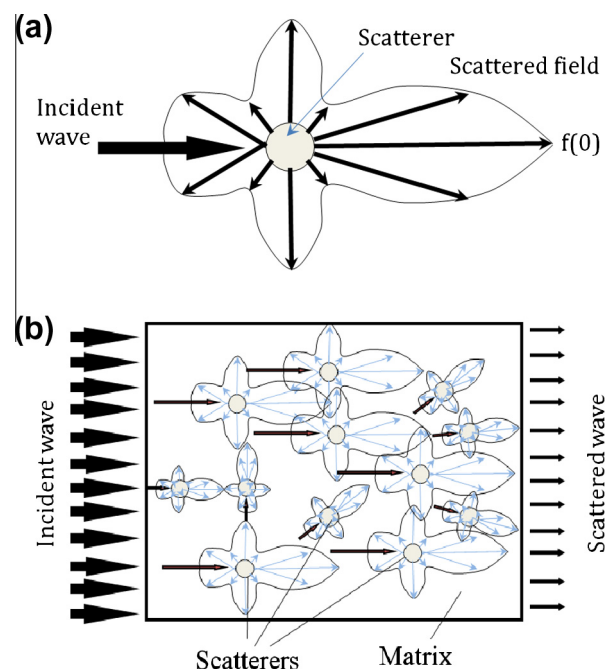


Fig. 4. (a) Scattering on a single void and (b) scattering on a matrix with randomly distributed voids.

material, while the measured density of the same reference material is 1969 kg/m³. The size of the scatterers used for the theoretical calculations was 3.9 mm, as mentioned earlier. Concerning their mechanical properties, the light particles were considered as cavities (bulk, shear moduli and density near zero).

Fig. 5 shows the phase velocity vs. frequency curves for different percentages of inclusions. As expected in scattering media, the dispersion curve is not a horizontal line; specifically it exhibits a minimum below 200 kHz. This minimum is more intense as the inclusion content increases. This is typical behavior of porous media [27] and the frequency of the minimum is defined by the typical size of the voids. In this case the local minimum of velocity is exhibited at the frequency of 160 kHz, where the wavelength (λ) is approximately 23 mm and the product of wavenumber ($k = 2\pi/\lambda$) times the inclusion size (R) is approximately equal to one:

$$k * R = \left(\frac{2\pi}{\lambda}\right) * R = 1.06 \quad (3)$$

In this regime ($k * R \approx 1$) the scattering interactions are strong [28]. This is another reason that the scattering model is used, as opposed for example for $k * R$ tending to zero, where the wavelength is orders of magnitude longer than the characteristic size of heterogeneity and homogeneous approaches are able to provide reasonable results. These results are compared to the experimental ones in the next section. It is mentioned that in similar media, approaches focusing on the incoherent part of the wave have also shown the potential to characterize distributed damage in the form of air voids or microcracking taking into account diffuse ultrasound and late wave arrivals [29,30].

4. Experimental results

4.1. Ultrasonics

Fig. 6a shows the experimental longitudinal wave velocity vs. the inclusion content. For plain material, the velocity is close to 3700 m/s a value quite usual for sound cementitious materials. For damage content up to 2.5% the velocity seems little influenced, while for higher content the velocity clearly decreases down to 3390 m/s. The red solid squares stand for the average of three specimens, while the dot lines represent the standard deviation. The velocity decrease incurred by damage is of the order of 10%. On the same graph, the theoretical values of longitudinal phase velocity are plotted, as taken for the frequency of 130 kHz from Fig. 5 (see arrow on horizontal axis of Fig. 5). This frequency is selected

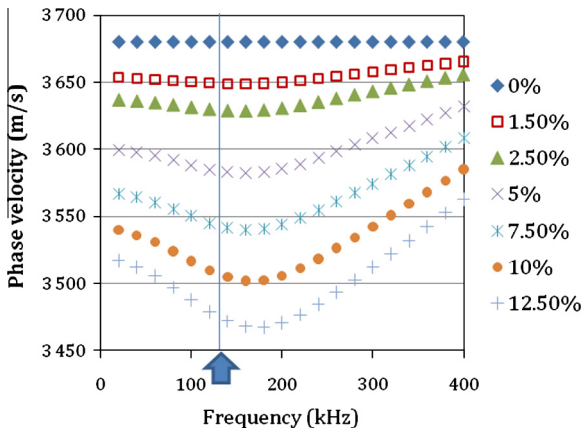


Fig. 5. Theoretical phase velocity vs. frequency curves for mortar with different volume content of cavities.

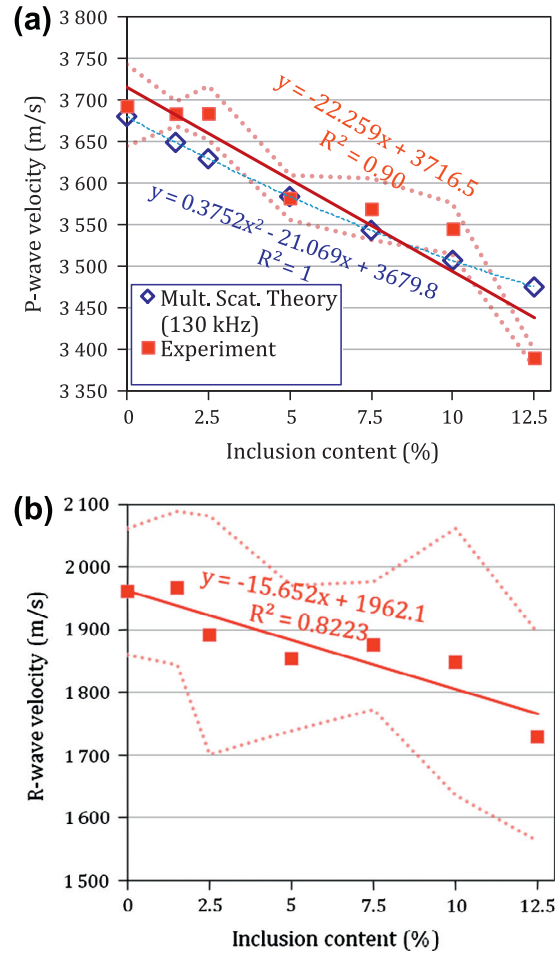


Fig. 6. Wave velocity vs. inclusion content: (a) longitudinal and (b) Rayleigh waves.

as the closest to the peak frequency of the received experimental signals (120–140 kHz). The agreement between the theoretical phase velocity and the experimental pulse velocity is good showing that the wave behavior of damaged concrete can be well simulated by scattering on material with cavities and the scattering contribution of sand is relatively negligible. This agreement shows that scattering should be used to explain the wave behavior of damaged cement-based materials in more detail than homogeneous approaches. As an example from Table 1, if the macroscopically homogeneous approach is followed for material G, the effective elastic modulus would be calculated at 18.9 GPa (given its wave velocity of 3390 m/s and its density of 1880 kg/m³). However, in reality this velocity measured at 130 kHz is the result of the existence of 12.5% of cavities of size 3.9 mm inside a cement matrix of 24.4 GPa, as shown by scattering theory.

In a theoretical basis (i.e. the scattering model in this case) when all but one parameters are fixed (size of scatterers, elastic properties, applied frequency, etc.) and only the value of volume content varies, there is one wave velocity value that corresponds to one specific volume content of scatterers ($R^2 = 1$ in Fig. 6a). Therefore, a simple inversion would lead to deterministic results; i.e. by knowing the wave velocity, the volume content would be calculated. When experiment is concerned, due to several “random” parameters this inversion cannot not provide similarly accurate results, so some differences in the theoretical and experimental curves of Fig. 6 arise (experimental $R^2 < 1$). Still in laboratory conditions most of the parameters can be controlled. So in the present case, since the volume fraction of scatterers is of interest, other mix design parameters like cement type, water

to cement ratio, aggregate to cement ratio, aggregate size distribution are kept constant. Therefore, a quite satisfactory inversion can be conducted despite the possible random experimental parameters that concern mixing, small differences in air content, etc. Under controlled conditions these inversions are possible. For example in the specific case, velocity values less than 3500 m/s indicate scatterer volume content of more than 10%. On the other hand velocities higher than 3650 m/s correspond to scatterer content lower than 5%. This characterization is certainly rough compared to the theoretical one-to-one inversion, but in an actual situation it would be very helpful and would contribute to the identification of the most vulnerable parts of a member given that other material parameters are similar (which is normal for a concrete belonging to the same batch).

The experimental surface (Rayleigh) wave velocity is depicted in Fig. 6b. Similarly to longitudinal, it exhibits a certain decrease with damage increase. The R-wave velocity exhibits a drop of more than 11% for inclusion-rich material showing that the influence of damage is at least equal in the Rayleigh mode, while the experimental scatter is also enhanced. Each dot is the average of 12 measurements on each type of material.

Scattering is a suitable way to explain the correlations between wave parameters and inclusion content since the wave physically propagates through the material and each inclusion/cavity leaves its fingerprint on the wave front. On the other hand, correlations with strength cannot be taken for granted, as the fracture of a material is a much more stochastic process. This is shown in Fig. 7 where the correlation of wave velocities vs. average load sustained on the bending test is depicted (“a” for longitudinal and “b” for Rayleigh). While most of the classes follow a reasonable trend, two of them (containing 5% and 10% of inclusions) exhibited a higher failure load than material with fewer inclusions and in overall they result in a non monotonic curve. Only the 12.5% material exhibits constantly lower strength and wave velocities of both modes.

An idea of the experimental scatter of the strength data is given in Fig. 8 which depicts the load of all 21 specimens (three for each class). The range of values for each class is typically around 0.3 MPa and the maximum range is 0.38 MPa for the 7.5% inclusion content. While a general decreasing trend is seen as the inclusion content increases, the trend cannot be regarded as monotonic since the 10% class exhibits the highest load bearing capacity in average. This is not unfamiliar to cementitious materials and mixtures, due to the inherent large variation of properties and mixing conditions. Although conglomeration of inclusions was not the case, it may have resulted by local variations on the amount of light inclusions. In the three point bending configuration, the maximum bending moment is exhibited in the mid-span. Therefore, the maximum load registered is a combination of the applied load, and the amount of reduction of the effective central vertical cross section due to the inclusions. Though the bending moment is sure to obtain its maximum value in the mid span due to geometry, the uniform reduction of the load bearing cross sections cannot be guaranteed, leading to some variability on the resulted maximum load. The fact that the 10% mortar surprisingly exhibited the highest load could have led to the decision to repeat the mix for this inclusion percentage. This would be the case if the only aim of the work was the correlation between ultrasonic velocity and inclusion content. However, one of our aims was to examine the possible correlation between AE parameters to failure load. Therefore, from this point of view there are seven classes of materials with different values of failure load and different AE parameters that exhibit the correlations which will be described later. Due to the physical existence of the inclusions that act as cavities, the wave velocity is influenced showing the corresponding decreasing trend of Fig. 6. However, due to the more complicated behavior at fracture, the existence of the total amount of light inclusions

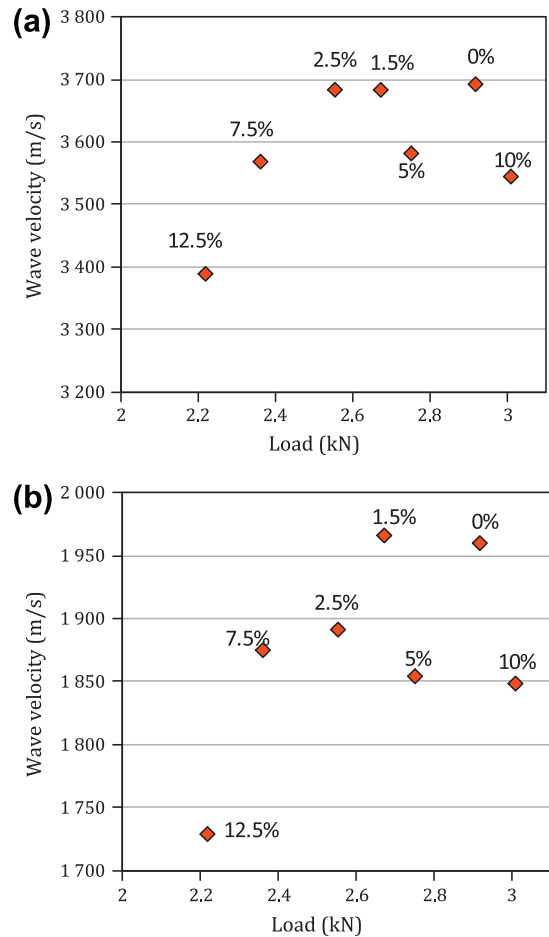


Fig. 7. Wave velocities vs. maximum bending load: (a) longitudinal, (b) Rayleigh (percentages on graph denote inclusion content).

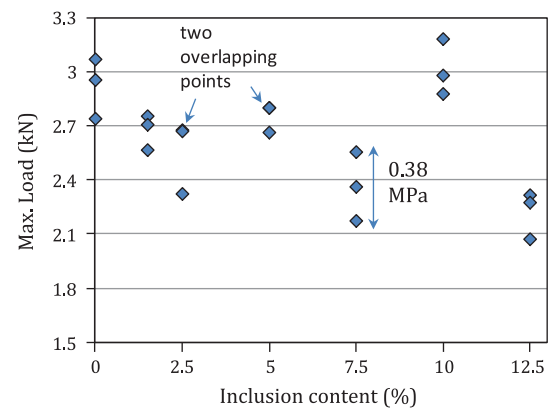


Fig. 8. Maximum load vs. inclusion content for all mortar specimens.

cannot guarantee the expected strength relatively to the more or less densely inclusion-populated specimens.

4.2. Acoustic emission results

At the moment of main fracture the tensile stresses at the bottom exceed the strength of the matrix material. The emitted signals from the fracture are recorded and their parameters analyzed. As aforementioned, frequency and waveform parameters are used for characterization of the severity of the process.

Specifically the following parameters are discussed herein: central frequency, defined as the centroid of the spectrum after fast Fourier transform (FFT) of each recorded waveform, measured in kHz and RA value which is inverse of the “rising angle” of the waveform and is defined as the ratio of rise time over the amplitude ($\mu\text{s}/\text{V}$) [9,10,12]. Additionally, the number of threshold crossings (counts) are of interest, while energy related parameters are also included since they have proven useful in monitoring of real structures [31]. In the present case RMS (root-mean-square – square root of the average of the squares of all points of a waveform) and ASL (the average signal level defined as the average amplitude of samples of the rectified signal [32]) are applied. Fig. 9a shows the maximum central frequency exhibited during the fracture of the specimens vs. the inclusion content. This feature monotonically decreases as inclusions increase and is characteristic of their scattering action. Actually the material of the specimens which is fractured under the bending load is the same mortar matrix regardless of the inclusion content. Therefore, a typical AE event should not systematically differ from specimen to specimen. Though the emissions from the fracture of the matrix are reasonable to be similar, the scattering action of the inclusions will certainly influence their propagation. Results of Fig. 9a show that the frequency received after a matrix crack may well differ by more than 100 kHz (20%) depending on the inclusion content of the material.

Additionally, the maximum RA recorded is seen in Fig. 9b. In general, RA value exhibits maxima at the moment of main crack formation [9,10] and it is related to the severity of the incident. In this case although, as mentioned earlier, the fracture events are not expected to differ in their source, the received signals exhibit a decreasing trend of RA as damage increases. This is again

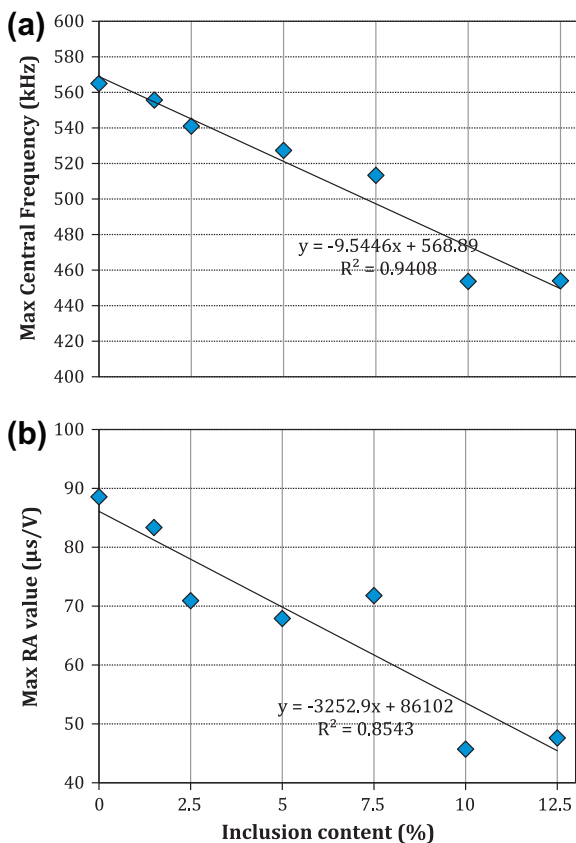


Fig. 9. AE parameters at the moment of fracture vs. the damage (inclusion) content of the material: (a) central frequency, (b) RA.

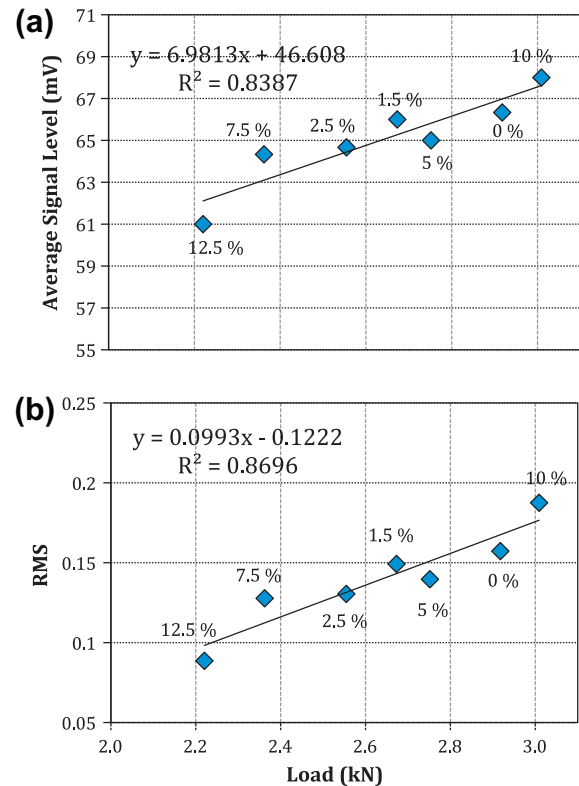


Fig. 10. (a) Average signal level and (b) root-mean-square vs. maximum load (percentages on graph denote inclusion content).

a result of the scattering action of the inclusions, which influences the amplitude of the signals, their duration and rise time and most of the waveform parameters possibly posing serious problems in AE classification as will be discussed.

As also examined for the ultrasonic parameters, correlations between AE parameters and failure load were sought. Since the failure load does not necessarily follow the increase of inclusion content, AE parameters well correlated to inclusions are not expected to correlate in the same way to the failure load. However, correlations exist, though not for the same AE indices which were found well correlated to simulated damage. These parameters are relative to the emitted energy, namely ASL and RMS, see Fig. 10a and b respectively. The straight curve fitting is just indicative of the clear increasing trend, showing that as the maximum load of the specimens increases, so do these AE energy indicators recorded by the sensors. This is reasonably connected to the released energy at fracture which depends on the load level. It is indicative that the RMS of the AE signals increases by a factor of two for material with the highest failure load (3.01 kN) compared to the lowest (2.22 kN). The same parameters are not similarly well correlated to the percentage of inclusions, showing that some parameters are suitable for correlation with existing damage or heterogeneity while others are more indicative of strength properties.

5. Discussion

In general, ultrasonic velocities are more successfully linked to inclusion content while AE energy parameters are linked to the failure load. However, due to their elastic nature, AE signals exhibit strong dependence on the inclusion content as well, mainly seen through RA value and central frequency. From the reported correlations of this study it seems that the strongest one is between the wave velocity and inclusion content, since the trend is monotonic

with a correlation coefficient R^2 higher than 0.9. Concerning failure load though, AE energy-related parameters seem to yield also strong correlations (R^2 just below 0.9). However, it would be premature to classify the different descriptors according to their characterization strength from this series of laboratory measurements. This mainly goes for the AE parameters, which are more sensitive than pulse velocity to the experimental conditions (sensor types, coupling, distance between crack and sensor). The importance is that AE parameters can be used in conjunction with slightly destructive tests, like the pull-out or drilling in order to supply extra correlations with the load bearing capacity of a material in a structure. So far several models have been proposed for compressive strength estimation based on ultrasonic pulse velocity and rebound hammer. Most of these provide relatively good results but they leave a substantial zone of uncertainty related to the specific material. Possible addition of another parameter (of the AE family this time) in a multiple parameter model will hopefully increase the accuracy provided by pulse velocity and is an area that needs serious future effort.

Although it can be argued that ultrasonic properties are physically related to elastic modulus, there is no certain relation between elasticity and strength (tensile, bending or compressive) so as to expect a robust correlation between UT results and failure load. In several cases, as already mentioned in the introduction, correlations may have emerged but these are empirical, while there is no proved physical connection between elasticity and the failure load of the specimen. Elastic modulus is the incremental resistance of a material to strain in the elastic region, while strength is defined by fracture criteria and the role of the material's microstructure (certainly smaller than the ultrasonic wavelength of some cm) is imperative. Therefore, it is reasonable that correlations to any type of strength should be sought for in the family of AE parameters, while existent damage in the form of cracks, voids, or inclusions which certainly influences the overall elastic properties should be better described by ultrasound propagation. In the specific case, the AE parameters are related to the bending strength of the material.

It is significant to highlight that up to a large extent the AE parameters depend on the texture of the material and not solely on the source. Despite the fact that AE sources are the same in all specimens since fracture starts from tensile cracks on the mortar matrix, several strong monotonic trends are noticed between AE parameters and damage content. This is particularly important since AE parameters are used for crack classification concerning the dominant fracture mode (tensile, mixed-mode or shear [9,12,33]). In any specific crack classification scheme the values of AE parameters including frequency indicators and RA are used to classify the events according to their source. Therefore, the differences presented due to heterogeneity can mislead characterization and misclassify the data.

The understanding of the different role of the two techniques is of paramount importance since it opens the direction for evaluating not only the content of damage which is one of the main goals of structural health monitoring but also the estimation of failure load which is the most crucial parameter for a load bearing construction.

6. Conclusions

This paper presents a combined study of elastic wave techniques on cementitious material with simulated damage. The main objective is to help in establishing tools for detailed assessment of the material's condition. Wave velocity can be quite accurately used to correlate to the damage content in the form of light spherical-like inclusions. Experiments are supported well by scattering theory, the results of which are in very good agreement for the

experimental frequencies. Additionally, the load bearing capacity of the specimens is tested. Though ultrasonic parameters do not exhibit similarly strong correlations with the ultimate load, specific parameters of AE seem to correlate better. This is reasonable since the ultimate load depends on the fracture incidents which are monitored through the emitted acoustic waves. Energy related parameters of AE reveal quite strong correlations directly to bending strength implying that apart from ultrasonic velocity which has been used for empirical correlations with strength, AE should be studied complementarily in order to improve the rough estimations of strength offered by ultrasonic velocity.

Acknowledgements

This research project has been co-financed by the European Union (European Regional Development Fund - ERDF) and Greek national funds through the Operational Program "THESSALY- MAINLAND GREECE AND EPIRUS-2007-2013" of the National Strategic Reference Framework (NSRF 2007-2013).

References

- [1] Naik TR, Malhotra VM, Popovics JS. The ultrasonic pulse velocity method. In: Malhotra VM, Carino NJ, editors. Handbook on nondestructive testing of concrete. Boca Raton: CRC Press; 2004.
- [2] Popovics S. Analysis of the concrete strength versus ultrasonic pulse velocity relationship. *Mater Evaluat* 2001;59(2):123–30.
- [3] Chaix JF, Rossat M, Garnier V, Corneloup G. An experimental evaluation of two effective medium theories, for ultrasonic wave propagation in concrete. *J Acoust Soc Am* 2012;131(6):4481–90.
- [4] Aggelis DG, Polyzos D, Philippidis TP. Wave dispersion and attenuation in fresh mortar: theoretical predictions vs. experimental results. *J Mech Phys Solids* 2005;53:857–83.
- [5] Treiber M, Kim JY, Qu J, Jacobs LJ. Effects of sand aggregate on ultrasonic attenuation in cement-based materials. *Mater Struct* 2010;43:1–11.
- [6] Vavva MG, Protopappas VC, Gergidis LN, Charalambopoulos A, Fotiadis DI, Polyzos D. Velocity dispersion of guided waves propagating in a free gradient elastic plate: application to cortical bone. *J Acoust Soc Am* 2009;125(5):3414–27.
- [7] Tsinopoulos SV, Polyzos D, Beskos DE. Static and dynamic BEM analysis of strain gradient elastic solids and structures. *CMES – Comput Modell in Eng Sci* 2012;86(2):113–44.
- [8] Grosse CU, Ohtsu M. Acoustic emission test. Springer; 2008.
- [9] Aggelis DG. Classification of cracking mode in concrete by acoustic emission parameters. *Mech Res Commun* 2011;38:153–7.
- [10] Farid Uddin AKM, Numata K, Shimasaki J, Shigeishi M, Ohtsu M. Mechanisms of crack propagation due to corrosion of reinforcement in concrete by AE-SiGMA and BEM. *Constr Build Mater* 2004;18:181–8.
- [11] Carpinteri A, Cardone F, Lacidogna G. Energy emissions from failure, phenomena: mechanical, electromagnetic, nuclear. *Experimental Mech* 2010;50:1235–43.
- [12] Ohtsu M. Recommendations of RILEM Technical Committee 212-ACD: acoustic emission and related NDE techniques for crack detection and damage evaluation in concrete: 3. Test method for classification of active cracks in concrete structures by acoustic emission. *Mater Struct* 2010;43(9):1187–9.
- [13] Schechinger B, Vogel T. Acoustic emission for monitoring a reinforced concrete beam subject to four-point-bending. *Constr Build Mater* 2007;21:483–90.
- [14] Aggelis DG, Mpalaskas AC, Ntalakas D, Matikas TE. Effect of wave distortion on acoustic emission characterization of cementitious materials. *Constr Build Mater* 2012;35:183–90.
- [15] Chaix JF, Garnier V, Corneloup G. Ultrasonic wave propagation in heterogeneous solid media: theoretical analysis and experimental validation. *Ultrasonics* 2006;44:200–10.
- [16] Aggelis DG, Momoki S. Numerical simulation of wave propagation in mortar with inhomogeneities. *Am Concr Inst Mater J* 2009;106(1):59–63.
- [17] Tsinopoulos SV, Polyzos D, Paipetis SA. Wave propagation in randomly cracked polymers, international symposium COMP 95. Greece: Corfu; 1995.
- [18] Lu Y, Liaw PK. Effects of particle orientation in silicon carbide particulate reinforced aluminum matrix composite extrusions on ultrasonic velocity measurement. *J Compos Mat* 1995;29:1096–116.
- [19] Abraham O, Piwakowski B, Villain G, Durand O. Non-contact, automated surface wave measurements for the mechanical characterisation of concrete. *Constr Build Mater* 2012;37:904–15.
- [20] Qixian L, Bungey JH using compression wave ultrasonic transducers, to measure the velocity of surface waves and hence determine dynamic modulus of elasticity for concrete. *Constr Build Mater* 1996;4(10):237–42.
- [21] Aggelis DG, Shiotani T. Experimental study of surface wave propagation in strongly heterogeneous media. *J Acoust Soc Am* 2007;122(5):151–7.

- [22] Waterman PC, Truell R. Multiple scattering of waves. *J Math Phys* 1961;2:512–37.
- [23] Foldy LL. The multiple scattering of waves. *Phys Rev* 1945;67:107–19.
- [24] Punurai W, Jarzynski J, Qu J, Kurtis KE, Jacobs LJ. Characterization of entrained air voids in cement paste with scattered ultrasound. *NDT and E Int* 2006;39:514–24.
- [25] Molero M, Segura I, Hernández MG, Izquierdo MAG, Anaya JJ. Ultrasonic wave propagation in cementitious materials: a multiphase approach of a self-consistent multiple scattering model. *Ultrasonics* 2011;51:71–84.
- [26] Ying CF, Truell R. Scattering of a plane longitudinal wave by a spherical obstacle in an isotropically elastic solid. *J Appl Phys* 1956;27:1086–97.
- [27] Sayers CM, Dahlin A. Propagation of ultrasound through hydrating cement pastes at early times. *Adv Cem-Based Mater* 1993;1:12–21.
- [28] Chekroun M, Le Marrec L, Abraham O, Durand O, Villain G. Analysis of coherent surface wave dispersion and attenuation for non-destructive testing of concrete. *Ultrasonics* 2009;49:743–51.
- [29] In Chi-Won, Brett Holland R, Kim Jin-Yeon, Kurtis KE, Kahn LF, Jacobs LJ. Monitoring and evaluation of self-healing in concrete using diffuse ultrasound. *NDT and E Int* 2013;57:36–44.
- [30] Schurra DP, Kim Jin-Yeon, Sabra KG, Jacobs LJ. Damage detection in concrete using coda wave interferometry. *NDT and E Int* 2011;44:728–35.
- [31] Shigeishi M, Colombo S, Broughton KJ, Rutledge H, Batchelor AJ, Forde MC. Acoustic emission to assess and monitor the integrity of bridges. *Constr Build Mater* 2001;15:35–49.
- [32] Kaewwaewnoi W, Prateepasen A, Kaewtrakulpong P. Measurement of valve leakage rate using acoustic emission. In: Proceedings of The ECT'05, pp. 597–600. May 12–13, Pataya, Chonburi, Thailand 2005.
- [33] Ohno K, Ohtsu M. Crack classification in concrete based on acoustic emission. *Constr Build Mater* 2010;24:2339–46.